Hindawi
Journal of Sensors
Volume 2021, Article ID 8870609, 12 pages
https://doi.org/10.1155/2021/8870609

Research Article

Development of a Multifunctional Radiation Measurement System for the Rapid Radiological Characterization of a Decommissioned Nuclear Facility Site

Han Young Joo,[1] **Jae Wook Kim**,[1] **Young Seo Kim**,[1] **So Yun Jeong**,[1] **Bongsoo Lee**,[2] **and Joo Hyun Moon**[1]

[1]*Department of Energy Engineering, Dankook University, 119, Dandae-ro, Dongnam-gu, Cheonan, Chungnam 31116, Republic of Korea*
[2]*Energy Systems Engineering, Chung-Ang University, 84 Heukseok-ro, Dongjak-gu, Seoul 06974, Republic of Korea*

Correspondence should be addressed to Joo Hyun Moon; jhmoon86@dankook.ac.kr

Received 20 July 2020; Revised 29 January 2021; Accepted 16 February 2021; Published 8 March 2021

Academic Editor: Marco Consales

In this study, a radiation measurement system with multifunctions for the rapid radiological characterization of a decommissioned nuclear facility site was developed and evaluated. The system remotely and simultaneously measures the beta and gamma radiation from the soil at a decommissioned nuclear facility site and wirelessly transmits the measurement data to the main server, which collects and analyzes the data. The radiation-measuring part of the system is composed of a sensing probe, multichannel analyzer (MCA), and laptop computer. The sensing probe is a phoswich radiation sensor (PHORS) consisting of two inorganic scintillators (NaI(Tl) and CaF_2(Eu)), each of which simultaneously measures the count rates and energies of the beta and gamma radiation. To test the performance of the PHORS, the beta and gamma radiation from a radiation source at 0–10 cm depths (at steps of 1 cm) under a soil surface was measured. The measurements show that the radiation count rates agree well with the theoretically predicted ones; the PHORS is as good as commercial radiation detectors in providing the energy spectrum of a radionuclide. In addition, a chi-square test was conducted, and the energy resolution was evaluated. The communication part of the system consisting of a global positioning system (GPS) and long-term evolution telecommunication (LTE) modem can successfully transmit the measurement data and their location information.

1. Introduction

The soil of a decommissioned nuclear power plant can be radioactively contaminated owing to leaks or the release of radioactive materials during its operation [1–3]. Radioactive contamination distributes and is found at different depths in the soil. The radionuclides frequently found in the soil at decommissioned nuclear sites are ^{60}Co, ^{90}Sr, ^{131}I, ^{137}Cs, thorium, uranium, and plutonium isotopes [4]. In addition, the soil at the TRIGA-MARK III site in Korea contained ^{51}Cr, ^{59}Fe, and ^{134}Cs [5].

If it is requested that a decommissioned nuclear facility site be released from regulatory controls, the radiation dose of the residual radioactivity at the site must be below the regulatory limits. The US Nuclear Regulatory Commission requires that the radiation dose from the residual radionuclides does not exceed 0.25 mSv/y for unrestricted release, whereas the Korean Nuclear Safety and Security Commission requires that the radiation dose does not exceed 0.1 mSv/y [6]. When evaluating the site release criteria of a decommissioned nuclear facility, a DCGL (derived concentration guideline level), which is a radionuclide-specific surface or volume residual radioactivity level that is related to a concentration or dose criterion, is usually applied [7].

To identify the radionuclides and their activity in the soil of a decommissioned site, in situ measurements with radiation detectors such as HPGe, NaI(Tl), and $LaBr_3$(Ce) detectors can be performed. Although these detectors measure with fair precision, they exhibit several deficiencies in in situ measurements. For example, they are not easy to use and too

Table 1: Properties of scintillators in PHORS.

	Density (g/cm^3)	Peak emission wavelength (nm)	Refractive index	Decay time (ns)	Light yield (photons/keV)	Relative rise time
NaI(Tl)	3.67	415	1.85	230	38	Fast
CaF_2(Eu)	3.19	395–435	1.47	940	19	Slow

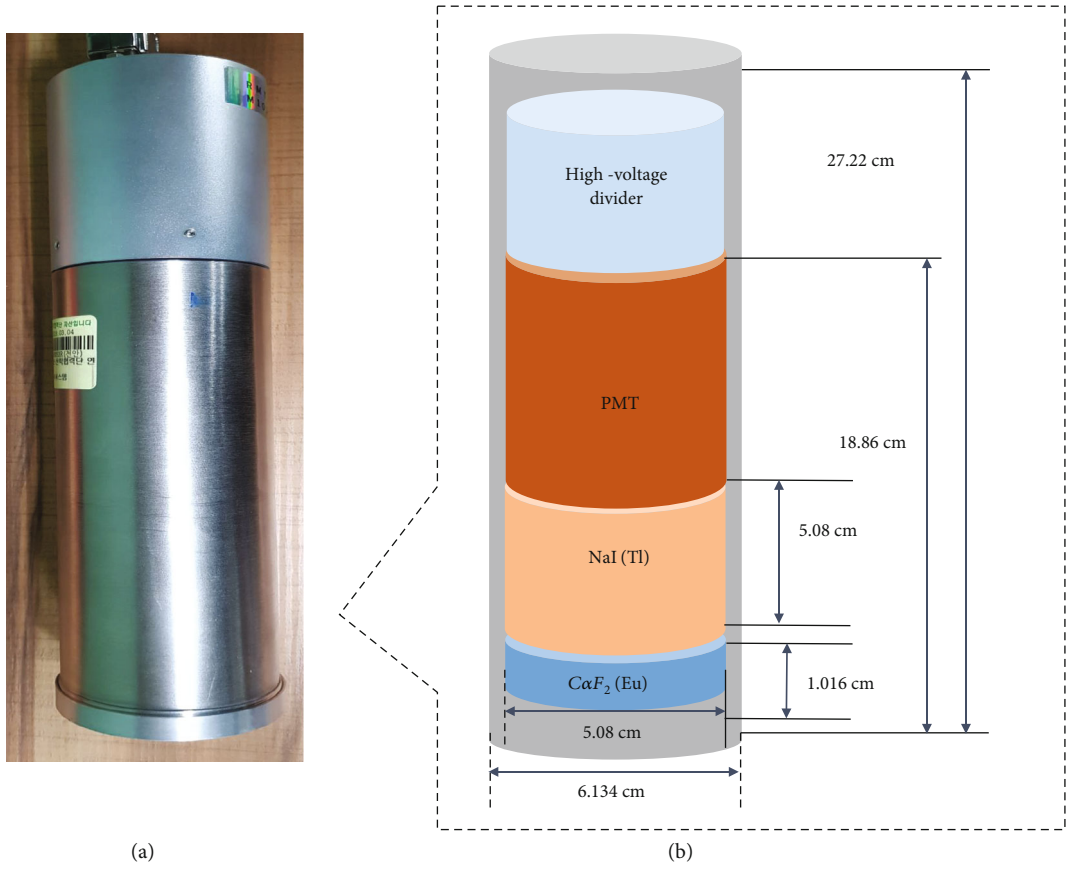

Figure 1: Photograph (a) and schematic (b) of PHORS.

bulky and heavy to be easily carried from one place to another within the site.

The soil samples can be analyzed ex situ in a separate location. Although this method provides high-precision results, it is labor intensive, induces secondary radioactive waste in the pretreatment and analysis of the sample, and requires time-consuming analyses. In particular, the analysis of low-energy beta emitters such as ^{14}C requires more time and labor. In addition, the reliability of the analysis results depends on the skill level of the analyst.

Researchers have investigated a variety of detectors that can simultaneously measure and analyze residual radionuclides in situ. To measure different types of radiation simultaneously, the detection materials are chosen considering the environment of the radiation measurement, radiation type to be detected, and interaction type. For example, a phoswich detector consists of a combination of two or more different scintillators. For the fabrication of a phoswich detector, two or more materials are selected depending on the emission wavelengths and decay/rise time properties. The resulting phoswich detector can separate the energies deposited on each scintillator.

Moghadmam et al. developed an alpha–gamma coincidence analysis device with a plastic and a CsI(Tl) scintillator [8]. Zorloni et al. simultaneously measured neutron and gamma rays with a scintillator and fiber optics [9]. In addition, Sánchez Del Río et al. developed a simultaneous detection system for protons and gammas by coupling two crystals [10], and Yamamoto and Ishibashi developed an alpha–beta–gamma simultaneous detection system with three different layers of scintillators [11]. However, none of these detectors can measure radiation remotely and transmit the measurement data wirelessly. Therefore, there is still room for improvement to provide a rapid and safe method for the characterization of a decommissioned nuclear facility site.

In this study, a radiation measurement system that remotely and simultaneously measures beta and gamma radiation from the soil was developed. This portable system is easy to use and quickly provides reliable energy spectra.

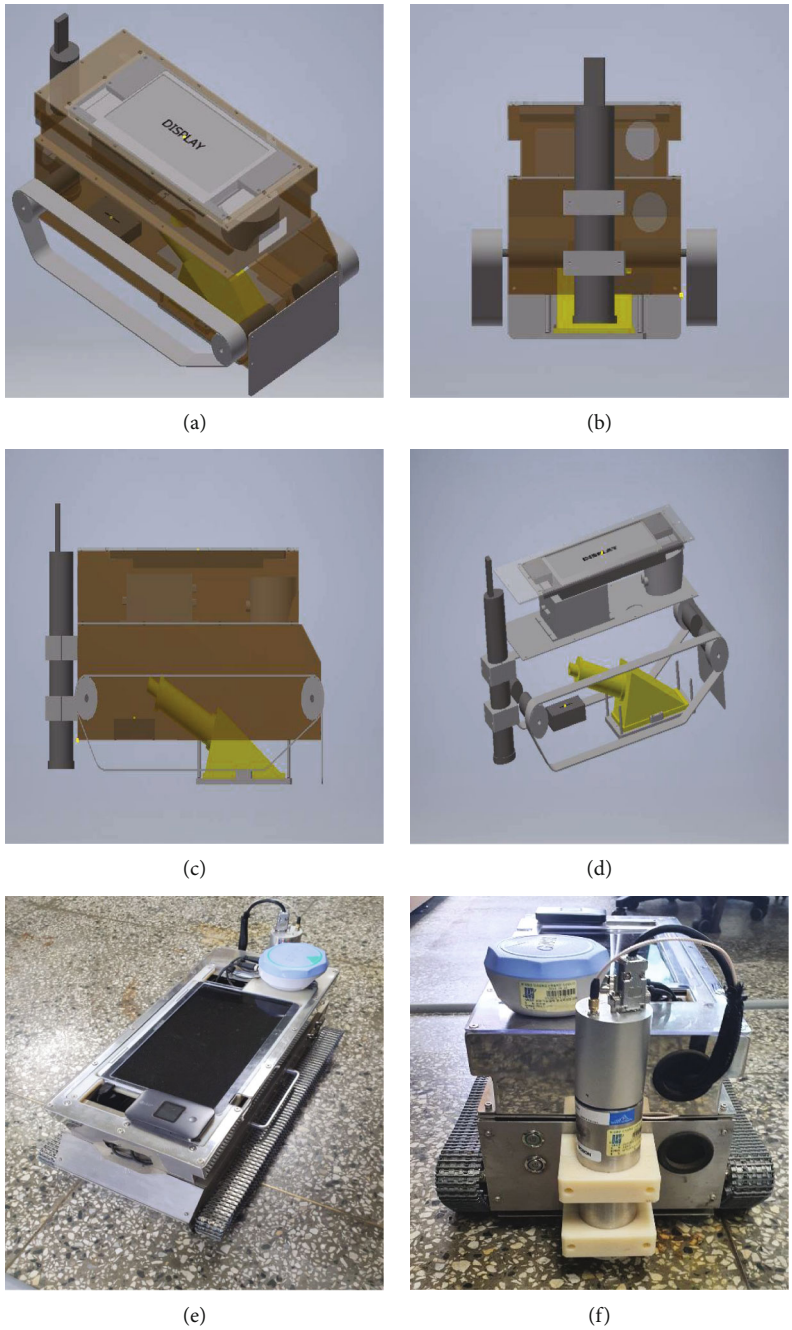

(a) (b) (c) (d) (e) (f)

Figure 2: Continued.

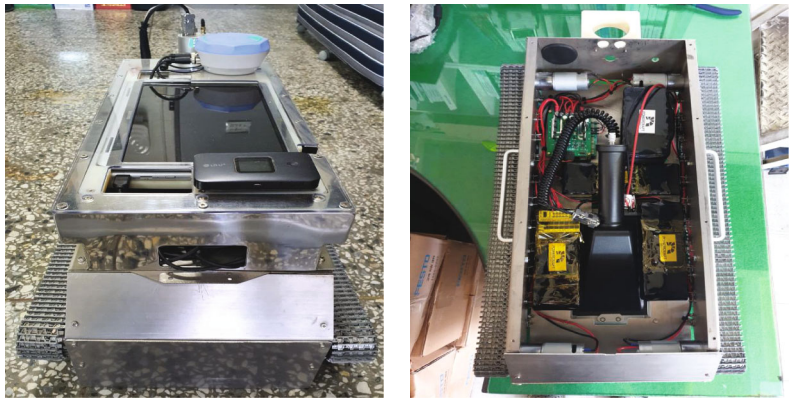

(g) (h)

Figure 2: 3D schematics (above) and photographs (below) of the complete measurement system: (a, e) the bird's eye view of the system, (b, f) the back of the system including the PHORS, (c) the side view, (g) the front, and (d, h) the interior.

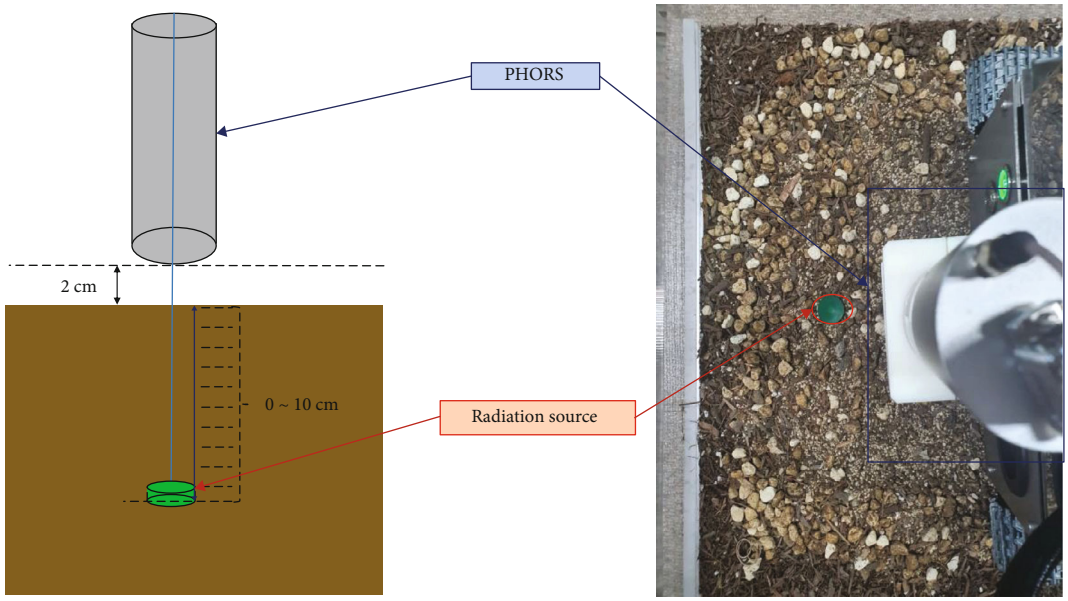

Figure 3: Experimental setup for measuring radiation from a radiation source in the soil.

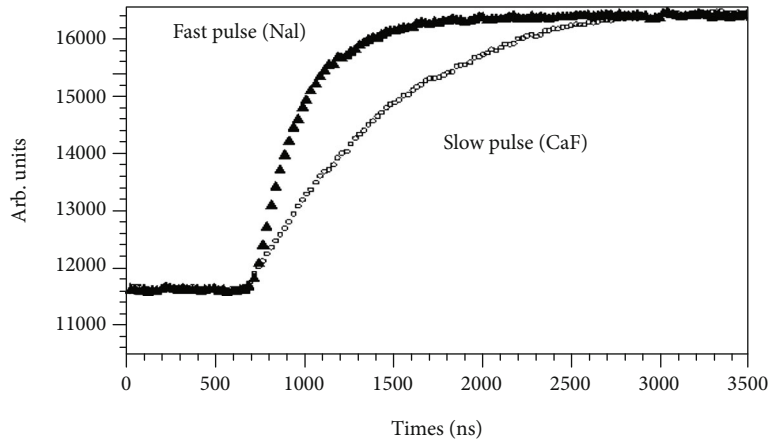

Figure 4: Examples of fast- and slow-rising pulses [12].

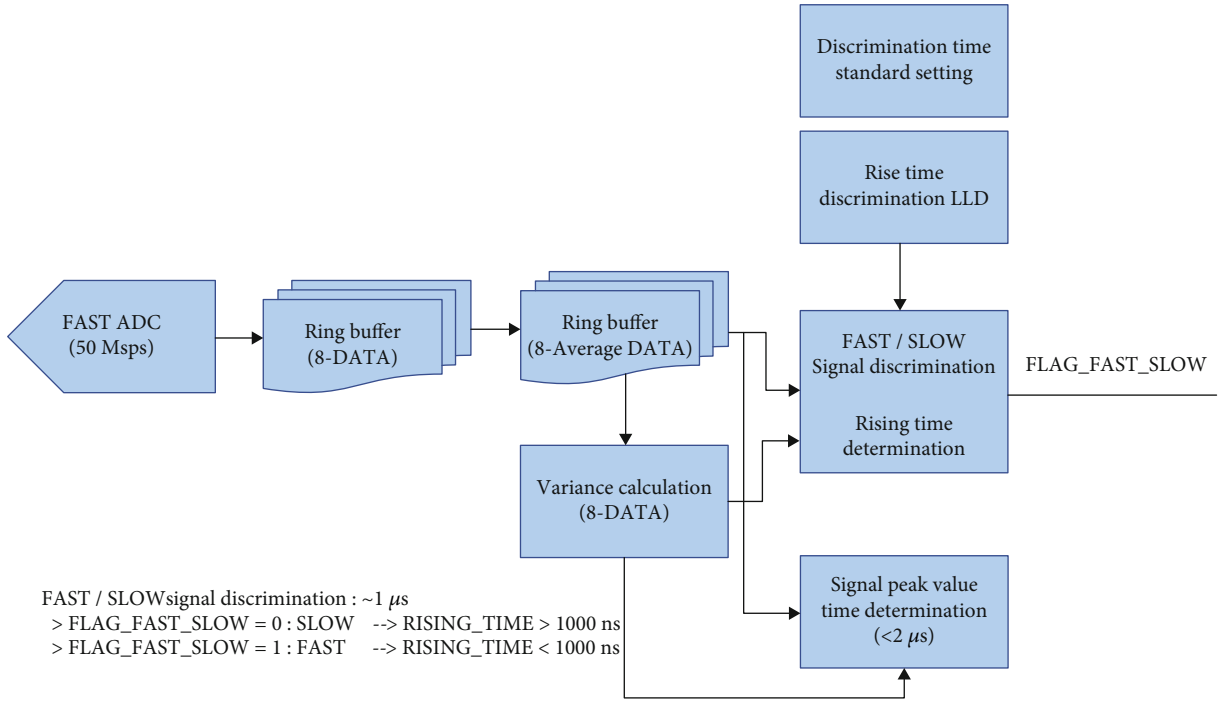

Figure 5: Process of discriminating the fast and slow signals.

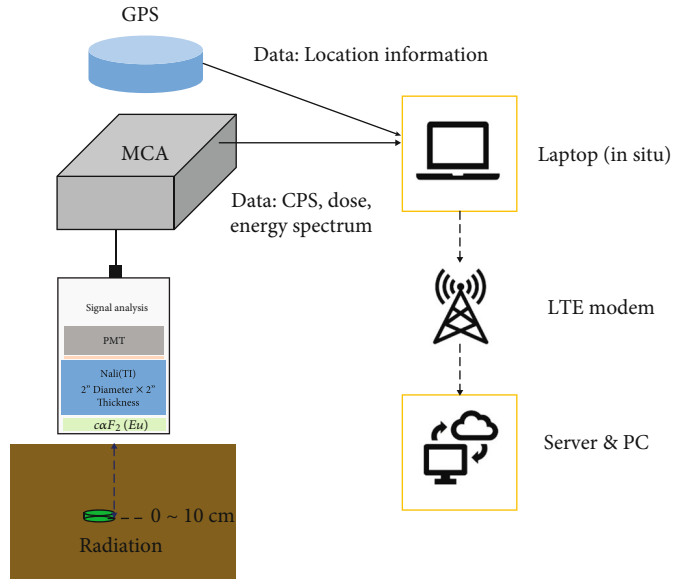

Figure 6: Data transmission between proposed radiation measurement system and main server.

Table 2: Radiological properties of radiation sources.

Radiation source	Shape	Current radioactivity (May 2020) (μCi)
^{60}Co	Thin disk	0.382
^{90}Sr	Thin disk	0.098
^{137}Cs	Thin disk	0.235

The radiation-measuring part of the system consists of a phoswich radiation sensor (PHORS), multichannel analyzer (MCA), and laptop computer. The communication part of the system consists of a global positioning system (GPS) and long-term evolution telecommunication (LTE) modem. The PHORS simultaneously measures beta and gamma radiation and identifies a radionuclide by analyzing the energy spectra. In addition, the system can wirelessly transmit measurement data to a server.

2. Materials and Methods

The PHORS probe was fabricated by combining two scintillators to enable the simultaneous measurement of beta

Table 3: Background radiation measurement results with PHORS probe.

Detector	Radiation type	Mean background rate (counts/s)	Mean total background (counts)	Critical level (counts)	Determination level (counts)
PHORS	Gamma	261.3	26134.4	376.7	26511.1
	Beta	10.3	1031.0	74.8	1105.8

and gamma radiation. An NaI(Tl) scintillator was used to measure gamma radiation. The inorganic scintillator has a high light output efficiency and wide emission range and the ease of fabricating large-sized crystals. Those characteristics help to reduce the sensitive volume required for the system and make compact arrangement inside the system. In the PHORS, the NaI(Tl) scintillator was placed into an aluminum casing, the thickness of which was minimized to consider the range of beta radiation. In addition, a CaF_2(Eu) scintillator was used to measure beta radiation. This scintillator has a relatively high light yield for beta rays, can be operated in a vacuum, and is chemically stable and robust to thermal and mechanical shocks. Table 1 summarizes the characteristics of the two scintillators. Moreover, Figure 1 shows a schematic and photo of the actual PHORS.

Figure 2 shows the entire measurement system including the PHORS; (a)–(d) present the 3D schematics and (e)–(h) show the photographs of the complete measurement system. Moreover, Figure 3 presents the experimental setup for measuring the radiation from an actual radiation source located at depths of 0–10 cm by 1 cm under the surface of the soil.

The red arrows in Figure 3 indicate the radiation source in the soil, and the dark blue arrows indicate the PHORS used to measure the radiation. The soil used in the experiment was a mixture of fertilizer and saprolite with leaf mold with a volume ratio of 1 : 1.

When gamma radiation reaches the PHORS, it passes through the CaF_2(Eu) scintillator and produces a fast-decay time and fast-rising pulse in the NaI(Tl) scintillator. By contrast, when beta radiation reaches the PHORS, it is deposited on the CaF_2(Eu) scintillator and produces a slow-decay time and slow-rising signal. The two distinct pulses can be seen in Figure 4 [12].

The light signal generated by the interaction between the radiation and scintillator is converted into an electrical signal by a photomultiplier tube (PMT, 9266B, ETI), which must be chosen considering the emission wavelength and have a refraction index that is identical to or approximately that of glass (≈1.5) for optimal coupling to the PMT's window. Consequently, the converted signal is distinguished by pulse shape discrimination (PSD) to distinguish between the differences in the rise times of the scintillators. Figure 5 shows the procedure in which the two signals are separated. The fast ADC (AD9649BCPZ-80, Analog Devices Inc.) with a sampling rate of 50 Msps acquires data in real time. The acquisition time for one dataset is 20 ns; thus, 50 datasets can be acquired in 1 μs. The FPGA circuit notices the start of the signal rise and automatically calculates the rise time. The rise time can be determined by the degree of dispersion of the data in the ring buffer. Finally, if the rise time is below 1 μs, the signal is fast; otherwise, the signal is slow. The relevant information is recorded and analyzed by the program installed on the laptop.

Table 4: Results of ^{60}Co source from PHORS measurements.

Depth* (cm)	^{60}Co Gamma (cps)**	^{60}Co Beta (cps)	Dose rate (nSv/h)
0	884.8 ± 28.0	61.7 ± 8.2	489.2 ± 7.7
1	715.6 ± 28.2	41.7 ± 7.1	389.6 ± 17.0
2	581.2 ± 22.6	28.2 ± 5.6	313.9 ± 1.9
3	548.5 ± 24.5	25.3 ± 4.8	296.4 ± 9.6
4	493.5 ± 22.2	21.1 ± 4.3	267.3 ± 3.7
5	455.0 ± 20.2	18.8 ± 4.4	246.5 ± 5.0
6	430.7 ± 22.0	18.3 ± 4.5	233.4 ± 6.2
7	413.3 ± 21.7	17.2 ± 4.0	223.9 ± 8.2
8	395.3 ± 20.4	16.9 ± 3.9	215.9 ± 3.3
9	384.7 ± 20.4	16.5 ± 4.3	209.7 ± 5.2
10	377.6 ± 19.9	16.8 ± 4.1	205.9 ± 5.4

*Distance from the soil surface. **Counts per second.

The proposed measurement system transmits the measurement data along with their location information through the LTE telecommunication network to the main server. Figure 6 shows the data transmission steps between the radiation measurement system and main server. Because the proposed measurement system can show the periodically updated measurement data and energy spectra of the gamma- emitters in real time, an operator can check the respective radiation level and easily identify any hot spots on site.

Three different thin-disk-type radiation sources (^{60}Co, ^{90}Sr, and ^{137}Cs) at 0–10 cm depths by 1 cm under the surface of the soil were measured five times for 100 s at each depth with the PHORS. Their radiological properties are listed in Table 2.

When a radiation source is measured, the radioactivity read by the detector is the sum of the natural radioactivity from the environment and that from the source. To determine only the contribution from the radiation source, the contribution of natural radioactivity must be extracted from the total radioactivity. The critical level is used to distinguish between the background radioactivity and radioactivity from the source [13].

$$L_c = 2.33 \times \sqrt{n_b}, \quad (1)$$

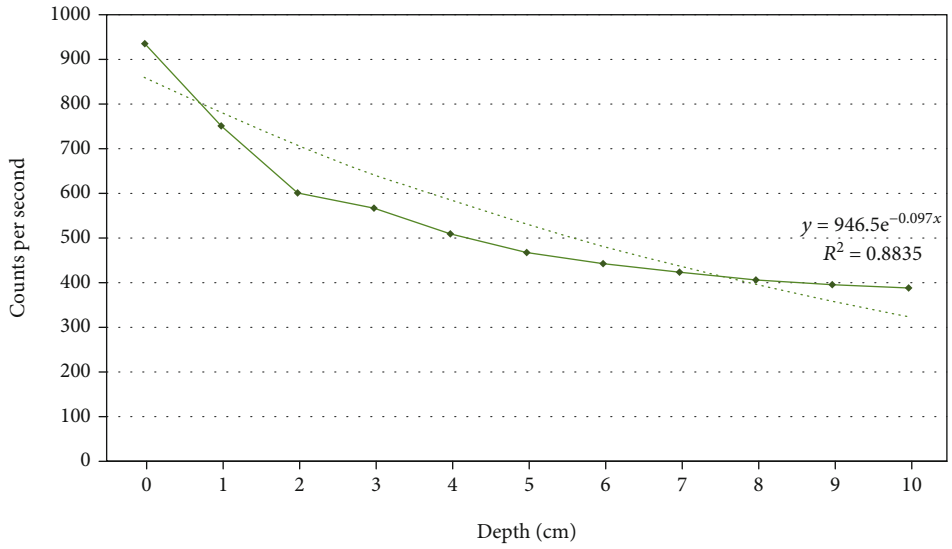

Figure 7: Results of ^{60}Co source from PHORS measurements.

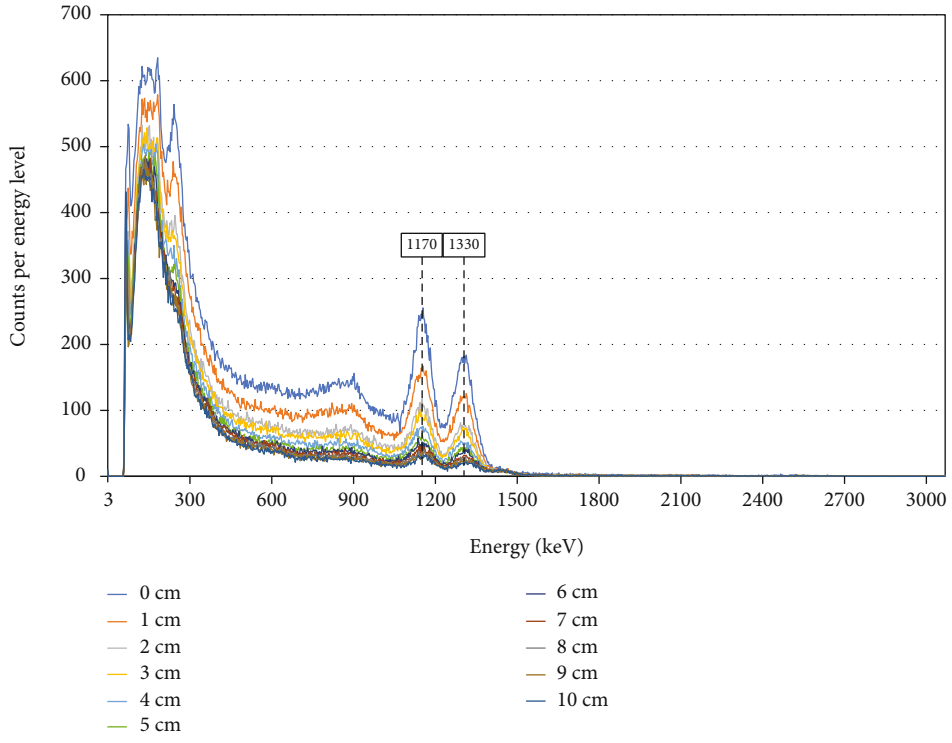

Figure 8: Energy spectra of ^{60}Co by depth using the PHORS.

where n_b is the background count. The determination level can be obtained by adding L_c to the background count. If the total count is less than the determination level, it can be assumed that the sample is not radioactive (with 95% confidence); if the total count exceeds the determination level, it can be assumed that the sample is radioactive (with 95% confidence) [14]. In this study, the PHORS probe was used to measure the background radiation for 100 s; subsequently, its critical level was determined.

3. Results and Discussion

To obtain the background count, the PHORS measured the background radiation five times for 100 s. As shown in Table 3, the gamma background count was 26134.4, and the critical level (L_c) was 376.7; the beta background count was 1031.0, and the critical level was 74.8. Consequently, the determination levels for the gamma and beta radiation were 26511.1 and 1105.8, respectively. These values were

Table 5: Results of ^{137}Cs source from PHORS measurements.

Depth* (cm)	^{137}Cs Gamma (cps)	^{137}Cs Beta (cps)	Dose rate (nSv/h)
0	880.7 ± 30.0	284.0 ± 18.3	600.4 ± 48.7
1	560.0 ± 24.1	27.9 ± 5.4	300.1 ± 31.1
2	452.3 ± 19.2	20.7 ± 4.7	246.5 ± 19.2
3	422.6 ± 19.4	19.7 ± 4.4	229.7 ± 4.5
4	390.4 ± 20.7	18.1 ± 4.2	213.9 ± 3.5
5	374.8 ± 19.5	16.3 ± 4.2	203.8 ± 8.3
6	354.4 ± 17.6	14.9 ± 3.6	194.6 ± 2.8
7	351.0 ± 18.4	14.4 ± 4.2	192.0 ± 3.3
8	334.9 ± 18.1	14.0 ± 3.6	184.4 ± 3.2
9	331.2 ± 16.6	13.9 ± 4.3	182.7 ± 3.3
10	324.8 ± 19.1	13.4 ± 4.0	178.6 ± 3.3

*Distance from the soil surface.

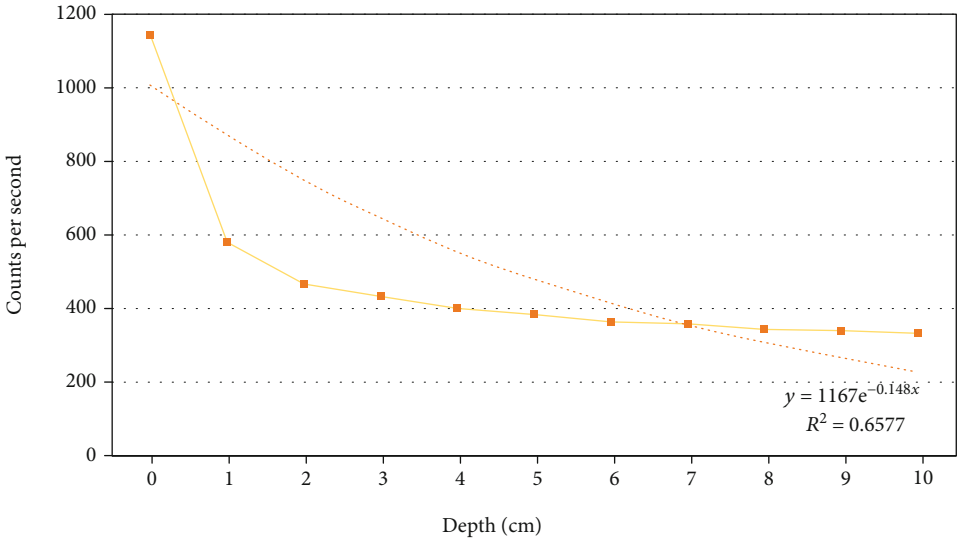

Figure 9: Results of ^{137}Cs source from PHORS measurements.

used as screening levels below which the total count in the subsequent measurement indicated a 95% probability that the sample was not radioactive. And the count rates were converted to the dose rates in nSv/h with the dose conversion factors for ^{60}Co, ^{90}Sr, and ^{137}Cs (ICRU-33).

Table 4 summarizes the results of the PHORS measurements. The uncertainties in Table 4 are $\pm 1\sigma$ (i.e., the standard deviation of the measurement results). Moreover, Figures 7 and 8 show the measurement results of the ^{60}Co source. The dotted curve in Figure 7 presents the theoretically expected reduction in the radiation intensity as a function of depth. Figure 8 shows the measured energy spectra at each depth. Thus, the PHORS can distinguish between the radiation energies.

Table 5 and Figure 9 summarize the experimental results for ^{137}Cs. In addition, the energy values from the measurements obtained using the PHORS at the depth of 0 cm were much higher than those at the other depths. A substantial portion of the total counts measured by the PHORS at the depth of 0 cm seems to be originated by three types of radiation from ^{137}Cs including two betas and one gamma ray. However, the contribution from the beta radiation to the total counts rapidly disappeared even at the depth of 1 cm or deeper. The energy spectra measured at each depth are presented in Figure 10 to evaluate whether the PHORS can distinguish between the radiation energies.

The most important factor in the energy measurement of radiation with a detector is the energy resolution; it indicates its capability to distinguish between the two nearest energies. When monoenergetic gamma or alpha radiation is measured, ideally, the energy spectrum measured by the detector should be a very sharp delta function. However, in reality, it would

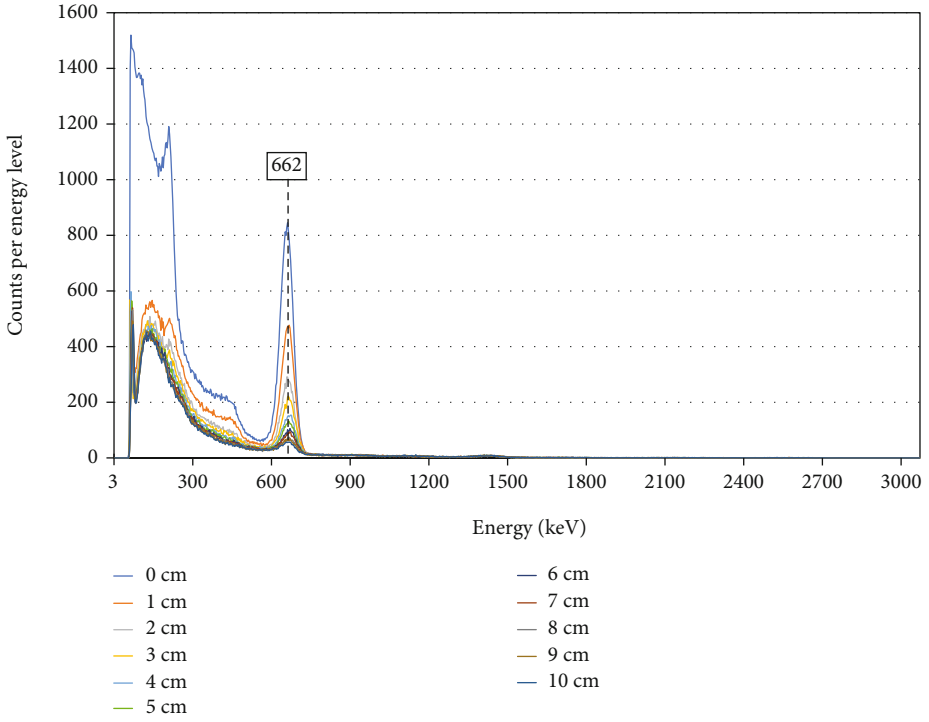

Figure 10: Energy spectra of ^{137}Cs with respect to depth measured with PHORS.

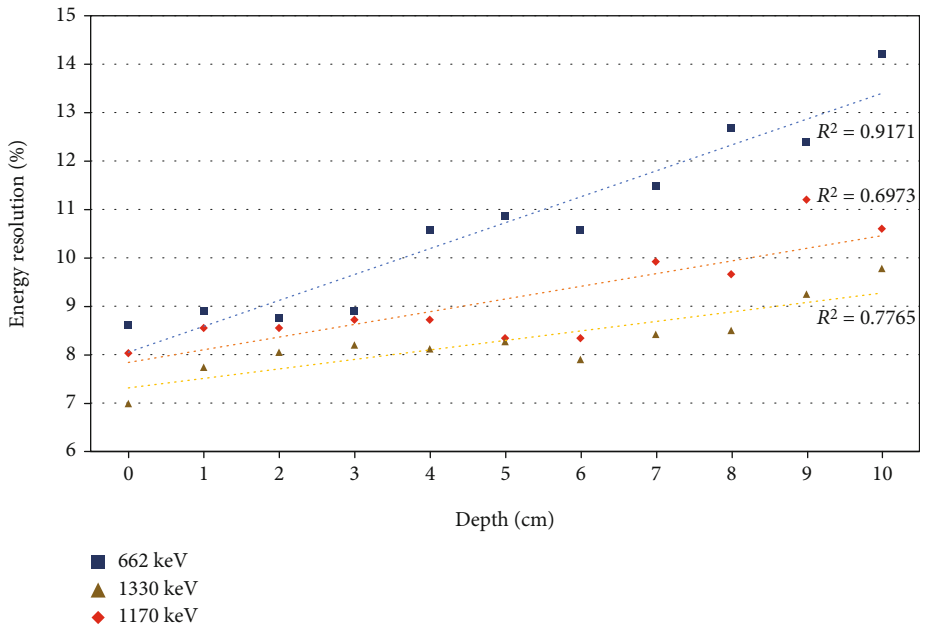

Figure 11: Energy resolutions of PHORS for ^{60}Co and ^{137}Cs with respect to depth.

be a peak in the form of a Gaussian function with finite width. This width is caused by fluctuations in the number of ionization and excitation events in the detector and could be produced by electronic parts such as an amplifier or MCA [15]. In general, the higher the energy is, the better the energy resolution is. In this study, the energy resolution at each depth was evaluated based on ^{60}Co and ^{137}Cs; ^{60}Co emits two gamma rays with 1170 and 1330 keV, and ^{137}Cs emits a gamma ray with 662 keV. The detector energy resolution is defined as follows:

$$R(\%) = \frac{\text{FWHM}}{E_0} \times 100, \quad (2)$$

Table 6: Results of ^{90}Sr source from PHORS measurements.

Depth* (cm)	Gamma (cps)	^{90}Sr Beta (cps)	Dose rate (nSv/h)
0	362.9 ± 8.2	443.4 ± 7.8	403.1 ± 49.3
1	266.6 ± 7.3	41.8 ± 3.2	163.2 ± 6.6
2	261.9 ± 8.2	13.1 ± 1.5	145.0 ± 5.5
3	261.5 ± 8.2	12.0 ± 1.5	146.7 ± 1.6

*Distance from the soil surface.

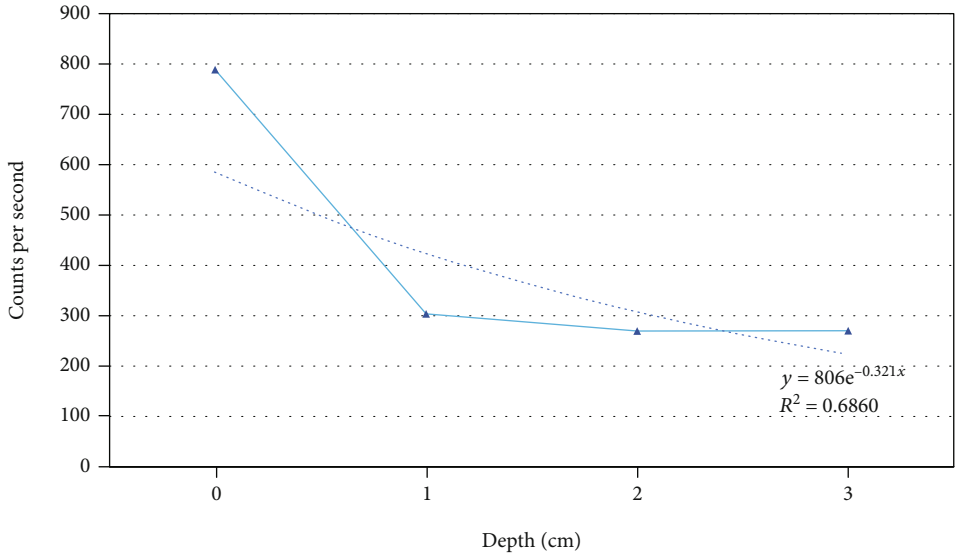

Figure 12: Results of ^{90}Sr source from PHORS measurements.

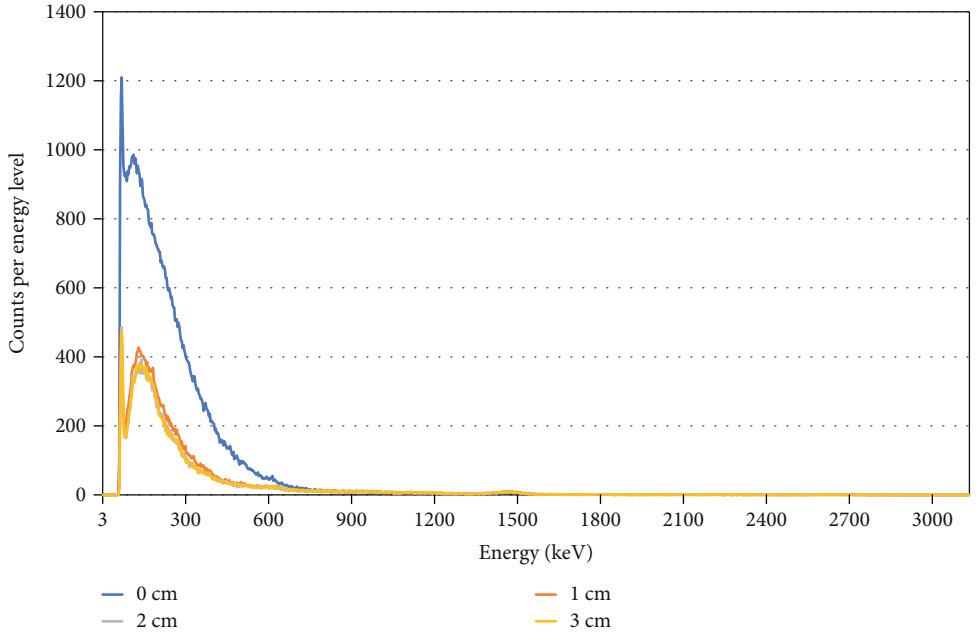

Figure 13: Energy spectra of ^{90}Sr with respect to depth measured with PHORS.

Table 7: Results of chi-square test for PHORS.

Depth (cm)	^{60}Co		^{137}Cs		^{90}Sr	
	χ^2	p value	χ^2	p value	χ^2	p value
0	220.1	0.91	255.1	0.38	217.1	0.92
1	276.6	0.11	259.0	0.32	263.5	0.24
2	218.9	0.92	203.5	0.98*	241.5	0.60
3	273.5	0.14	220.8	0.90	217.0	0.92
4	248.1	0.50	273.4	0.14		
5	224.1	0.87	252.5	0.43		
6	278.6	0.10	216.9	0.93		
7	283.4	0.07	239.8	0.65		
8	262.3	0.27	244.4	0.57		
9	269.6	0.18	206.9	0.98*		
10	261.4	0.28	279.3	0.09		

*Outliers.

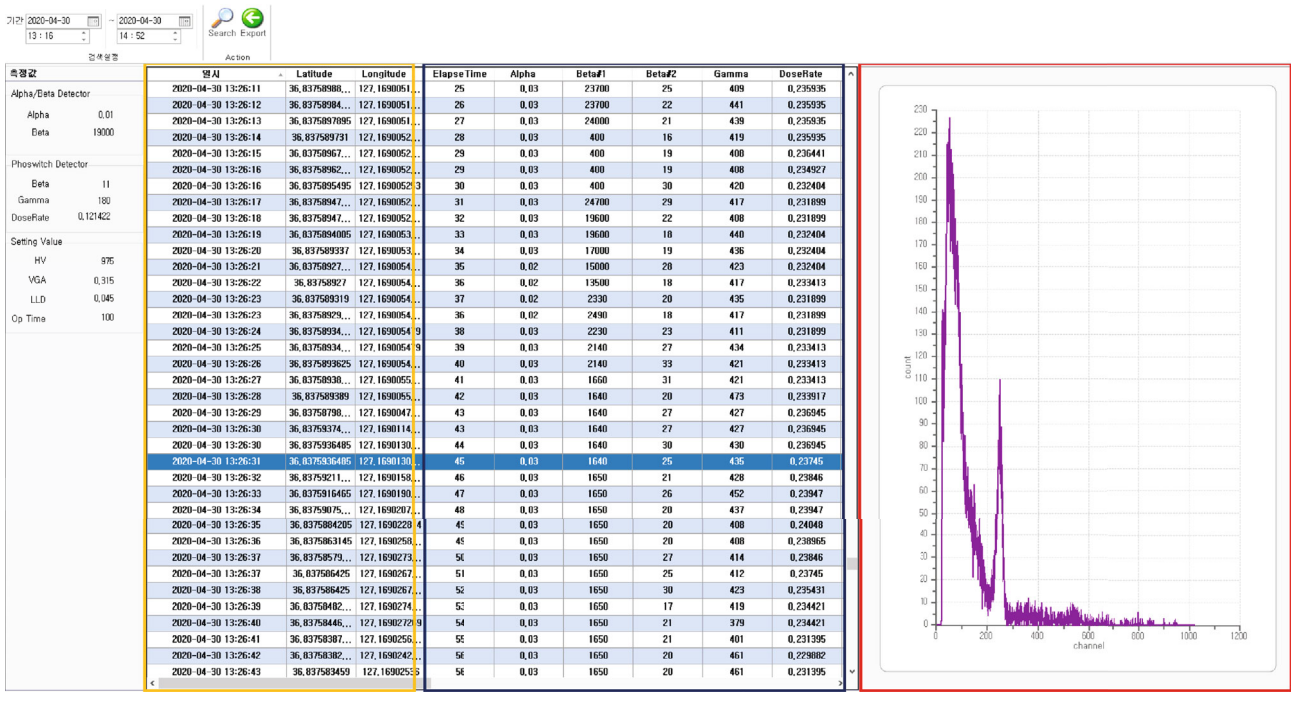

(a) (b) (c)

Figure 14: Example of past measurement data: (a) time and location information; (b) alpha, beta, and gamma measurements in cps and dose rate; and (c) noncalibrated energy spectrum.

where R is the energy resolution, FWHM the full-width at half-maximum, and E_0 the energy of the peak centroid. Scintillation detectors used for gamma ray spectroscopy normally show energy resolutions in the range of 3% to 10% [13]. Figure 11 shows the energy resolutions for each depth and radiation source. According to Figure 11, the energy resolution of the PHORS was less than 10%, which is approximately identical to that of the commercial gamma detectors. However, because the ^{137}Cs source was deeper than 4 cm below the surface, the PHORS energy resolution exceeded 10%.

By contrast, the energy range of beta radiation is much shorter than that of gamma radiation; consequently, the depth at which the PHORS could detect the beta radiation was very shallow compared to that of the gamma radiation. Therefore, the ^{90}Sr measurements were only performed at four different depths. Table 6 and Figures 12 and 13 present the experimental results for ^{90}Sr.

Because the measurement results at 0–3 cm depth exceeded the determination level (Table 3), it can be assumed that the PHORS can detect radiation from a source with 95% confidence. However, if the source is located at 4 cm depth or

deeper, the PHORS cannot statistically distinguish the radiation from the source from the natural one.

To evaluate statistically the reliability of the PHORS, a chi-square test (χ^2 test) was performed with the following equation:

$$\chi^2 \bullet = \frac{\sum(\bar{x} - x_i)^2}{\bar{x}}, \quad (3)$$

where $\bar{x}$ is the mean of all the measurements and x_i is the value of the ith individual measurement. Table 7 shows the results of the chi-square tests for ^{60}Co, ^{90}Sr, and ^{137}Cs. If the p value is between 0.05 and 0.95, it can be concluded that the detector worked as expected. According to Table 7, most p values are between 0.05 and 0.95 except for only two cases, which means that PHORS generally provide statistically reliable measurements.

Figure 14 shows an example PC screen with the measurement results from the system ((a) measurement results, (b) GPS information, and (c) noncalibrated energy spectrum).

4. Conclusions

In this study, a remote wireless measurement system was developed to detect simultaneously beta and gamma radiation from the soil at a decommissioned nuclear site. The measurement system is composed of a sensing probe, MCA, and laptop computer. The sensing probe is a PHORS consisting of inorganic scintillators (NaI(Tl) and CaF_2(Eu)), each of which simultaneously measures the count rates and energies of the beta and gamma radiation. The performance of the PHORS was evaluated by measuring three different radiation sources at different depths under the soil surface. The results show that the PHORS can produce statistically reliable measurements and provide energy spectra that can be used to identify the radionuclide of interest. Moreover, the communication part of the system (which consists of a GPS and an LTE modem) can transmit the measurement data and their location information. The proposed measurement system was successfully applied to measure a combination of beta and gamma emitters often found at decommissioned nuclear facility sites with a significantly reduced measurement time; thus, the device improves worker safety by limiting their exposure to residual radiation. In the future, real radiation field tests must be conducted, and a more controlled experimental environment must be created to compare the experimental results with simulations.

Data Availability

We can provide the data if requested.

Conflicts of Interest

The authors declare that there is no conflict of interest regarding the publication of this paper.

Acknowledgments

This work was supported by the National Research Foundation of Korea (NRF) grant funded by the Korea government (Ministry of Science and ICT) (No. 2020M2D2A2062436).

References

[1] B. Lukšiene, D. Marčiulioniene, I. Gudeliene, and F. Schönhofer, "Accumulation and transfer of ^{137}Cs and ^{90}Sr in the plants of the forest ecosystem near the Ignalina Nuclear Power Plant," *Journal of Environmental Radioactivity*, vol. 116, pp. 1–9, 2013.

[2] M. Mizoguchi, "Monitoring of soil radiation doses from contaminated soil buried in a paddy field in Iitate Village, Fukushima," *Paddy and Water Environment*, vol. 17, no. 2, pp. 299–302, 2019.

[3] H. W. Lee, J. Y. Kim, and C. L. Kim, "Study on the experiences of subsurface soil remediation at commercial nuclear power plants in the United States," *Journal of Nuclear Fuel Cycle and Waste Technology(JNFCWT)*, vol. 17, no. 2, pp. 213–226, 2019.

[4] L. E. Boing, *Introduction to Decommissioning*, Argonne National Laboratory, 2013.

[5] K. G. Kim, H. J. Won, and W. Z. Oh, "Methods of recycling soil washing wastewater for volume reduction," *Journal of Soil and Groundwater Environment*, vol. 8, no. 1, pp. 17–26, 2003.

[6] US Nuclear Regulatory Commission, *10 CFR Part 20*, US Nuclear Regulatory Commission, 2015, http://www.nrc.gov/reading-rm/doc-collections/cfr/part020/index.html.

[7] K. W. Lee, S. B. Hong, J. H. Park, and U. S. Chung, "Final status of the decommissioning of research reactors in Korea," *Journal of Nuclear Science and Technology*, vol. 47, no. 12, pp. 1227–1232, 2010.

[8] S. R. Moghadam, S. A. H. Feghhi, and M. J. Safari, "A phoswich detector for simultaneous alpha-gamma spectroscopy," *Nuclear Instruments and Methods in Physics Research*, vol. 799, pp. 59–63, 2015.

[9] G. Zorloni, F. Cova, M. Caresana et al., "Neutron/γ discrimination by an emission-based phoswich approach," *Radiation Measurements*, vol. 129, p. 106203, 2019.

[10] J. S. del Río, M. Mårtensson, M. J. G. Borge et al., "CEPA: ALaBr3(Ce)/LaCl3(Ce)phoswich array for simultaneous detection of protons and gamma radiation emitted in reactions at relativistic energies," *EPJ Web of Conferences*, vol. 66, p. 11033, 2014.

[11] S. Yamamoto and H. Ishibashi, "Development of a three-layer phoswich alpha-beta-gamma imaging detector," *Nuclear Instruments and Methods in Physics Research*, vol. 785, pp. 129–134, 2015.

[12] J. H. Ely, C. E. Aalseth, and J. I. McIntyre, "Novel beta-gamma coincidence measurements using phoswich detectors," *Journal of Radioanalytical and Nuclear Chemistry*, vol. 263, no. 1, pp. 245–250, 2005.

[13] G. F. Knoll, "Ch. 3: limits of detectability," in *Radiation Detection and Measurement*, John Wiley & Sons, New Jersey, 4th edition, 2010.

[14] L. A. Currie, "Limits for qualitative detection and quantitative determination: application to radiochemistry," *Analytical Chemistry*, vol. 40, no. 3, pp. 586–593, 1968.

[15] G. F. Knoll, "Ch. 2: interaction of heavy charged particles," in *Radiation Detection and Measurement*, John Wiley & Sons, New Jersey, 4th edition, 2010.